The $\bar{\text{P}}$ANDA experiment at FAIR

The $\bar{\mathrm{P}}$ANDA experiment at FAIR

Tord Johansson

Dept. of Physics and Astronomy, Uppsala University, Box 516, SE-75126 Uppsala, Sweden for the $\bar{\mathrm{P}}$ANDA Collaboration

E-mail: tord.johansson@physics.uu.se

Abstract. The Facility for Antiproton and Ion Research, FAIR, is presently under construction near Darmstadt, Germany. Among other large-scale installations, the $\bar{\mathrm{P}}$ANDA (Antiproton annihilations in Darmstadt) experiment is designed to address pertinent questions of the strong interaction in the non-perturbative region. At $\bar{\mathrm{P}}$ANDA, an antiproton beam, with momenta between 1.5 GeV/c and 15 GeV/c, circulating in the high-energy storage ring HESR will interact with internal targets. High interaction rates and unprecedented momentum resolution will allow for a high discovery potential and precision experiments. The detector system of $\bar{\mathrm{P}}$ANDA is optimised to meet the challenges of high-resolution hadron spectroscopy in formation and production with very good background suppression. At the same time, it meets the requirements of other parts of the physics program such as hyperon and hadron structure physics. The detector is reviewed and physics goals are presented.

1. Introduction

FAIR is an international multipurpose facility that will provide stable beams from protons up to uranium over a wide range of energies and intensities as well as intense high-quality secondary beams of antiprotons and radioactive isotopes. The physics program that will be conducted at FAIR is based of four scientific pillars: NUclear STructure Astrophysics and Reactions by the NUSTAR collaboration, Compressed Baryonic Matter studies formed in relativistic heavy ion collisions by the CBM collaboration; Atomic, Plasma Physics and Application studies by the APPA collaboration and hadron physics studies by the $\bar{\mathrm{P}}$ANDA collaboration. For a more detailed presentation of FAIR and NUSTAR, CBM and APPA see the contribution from P. Giubellino in these proceedings. The $\bar{\mathrm{P}}$ANDA experiment will use antiprotons that are produced by 29 GeV protons impinging on a metallic production target. Antiprotons with an energy of about 3 GeV will be transferred to a Collector Ring where they will be cooled and accumulated before being transferred to the racetrack-shaped High Energy Storage Ring (HESR) where they are further cooled and accelerated/decelerated to the desired energy. The $\bar{\mathrm{P}}$ANDA experiment is located at one of the straight sections of HESR. Two operation modes of HESR are foreseen: 1) a high-luminosity mode with a peak luminosity of $2 \cdot 10^{32} cm^{-2} s^{-1}$ and 2) a high-resolution mode with a momentum spread, $\Delta p/p$, of the order of 10^{-5} with an order of magnitude lower luminosity. These excellent features, in combination with the $\bar{\mathrm{P}}$ANDA detector, will allow for unprecedented investigations of the strong interaction in the non-perturbative region of the strong interaction and test of fundamental symmetries.

2. The $\bar{\text{P}}$ANDA detector.

The $\bar{\text{P}}$ANDA detector [1] is depicted in Figure 1. It consists of a Target Spectrometer (TS) and and Forward Spectrometer (FS) with an excellent coverage of $\sim$ 90% of the solid angle. The construction of the detector will be staged and Fig.1 shows the detectors that are foreseen for the Day 1 and Day 2 stages.

The TS is a layered detector built inside a superconducting solenoid that provides a magnetic field of 2T. $\bar{\text{P}}$ANDA will equipped with a cluster jet target for Day 1 with beams of hydrogen, deuterium and noble gases. For tracking, will the interaction point be surrounded by a Micro Vertex Detector (MVD) made from silicon pixels and strips. The MVD is surrounded by a Straw Tube Tracker (STT) and one layer of a Gas Electron Multiplier detector (GEM) in the forward direction. These detectors provide a transverse momentum resolution of 1.5%. Particle identification (PID) in the TS of pions, kaons and protons will be done *via* $\Delta E/E$ information from the STT, a Barrel Time-of-Flight (ToF) system made from scintillator pads and a Barrel DIRC (Detection of Internally Reflected Cherenkov light). Interleaved Muon Chambers made from streamer tube detectors in the magnetic yoke will identify muons. Photon and electron detection is achieved in an Electromagnetic Calorimeter (EMC) made from PWO_4 crystals.

The FS is arranged along the beam line and covers the polar angles $\pm 10°$ and $\pm 5°$ horizontally and vertically, respectively. A Dipole Magnet (DM) with an integral field of up to 2 Tm is a part of the HESR lattice and is equipped with layers of STT chambers of similar design as the TS STT for tracking. PID is made via a ToF system made from scintillator slabs. Photons and electrons are measured in a Shashlyk detector, followed by a muon range system of a similar design as the TS.

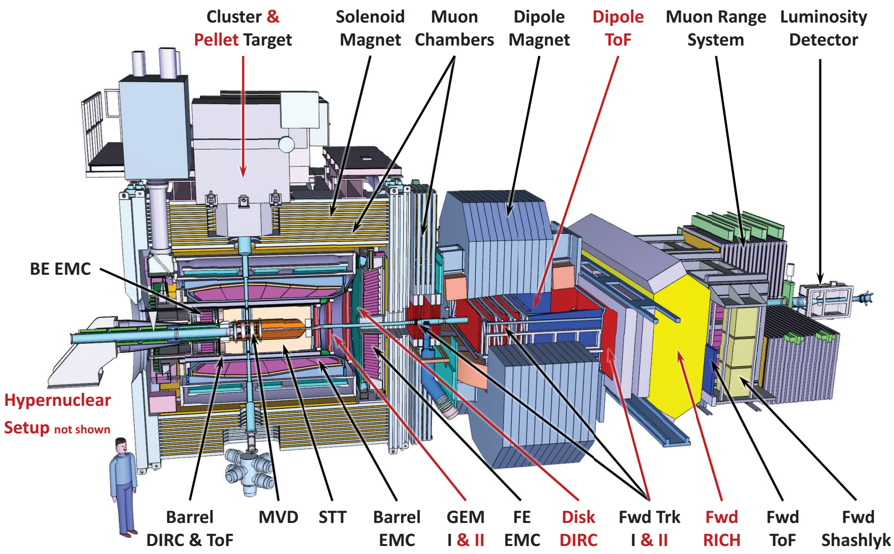

Figure 1. The $\bar{\text{P}}$ANDA detector. The detectors that are planned for Day 1 are labelled in black, whereas the additional detectors foreseen for Day 2 are labelled in red.

A luminosity detector is located downstream of the FS made from HV-MAPS pixel silicon detectors to measure elastically scattered antiprotons. It will provide an absolute luminosity measurement of 5 % and a relative measurement of 1 %.

For Day 2 set-up will the TS be completed with a pellet target system, two additional layers of GEM detectors and a planar Disc DIRC detector in the forward direction. The FS will be completed with an additional ToF detector in the DM and additional STT tracker planes after the DM plus a RICH detector for PID. A target system with dedicated instrumentation for hypernuclear physics will also be made available.

3. The PANDA experimental program

The momentum range of HESR allows for invariant masses of up to 5.5 GeV/c^2 to be produced in antiproton-proton collisions. This is illustrated in Figure 2 where also two-body thresholds are indicated. As can be seen, all strange hyperons and single charm hyperons, charmonium and open strange ($D\bar{D}$) meson are accessible in this momentum region.
Antiproton-proton collisions are very advantageous for spectroscopy studies since all quantum numbers that are allowed for $q\bar{q}$ states are accessible in formation and and high spin states are readily produced.This is in contrast to e^+e^- collisions which predominantly populate states with $J^{PC} = 1^{--}$. States with exotic quantum numbers, which must contain a gluonic component, can be produced in production processes. The region above the $D\bar{D}$ threshold is an excellent hunting ground for of exotic states containing charm quarks and glueballs. A more comprehensive review than given here can be found in Refs [2, 3]

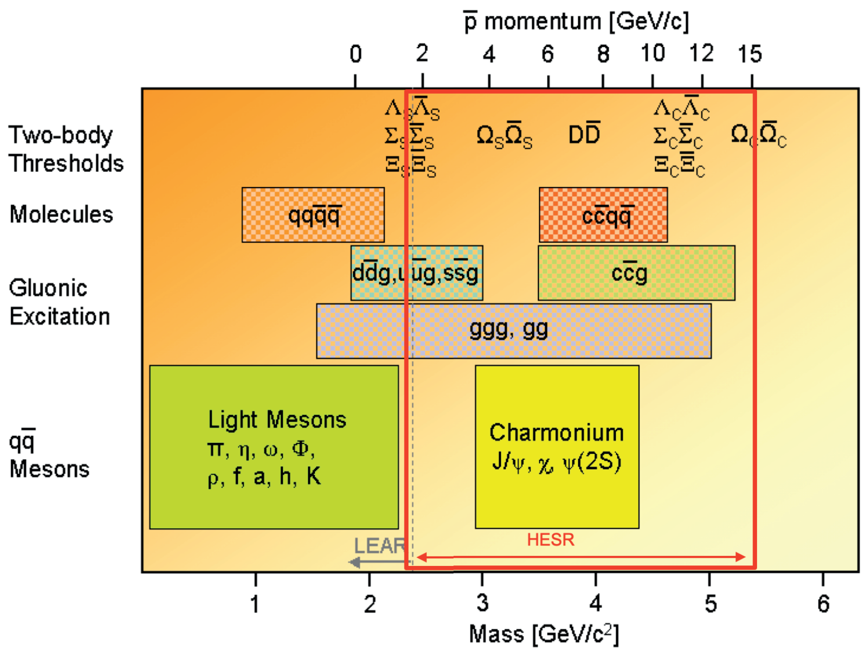

Figure 2. The mass range covered by HESR in formation. Two-body thresholds in formation are indicated as well as expected mass ranges for exotics.

3.1. *Charm and exotics*

The charm sector is of particular interest for spectroscopy due to the narrowness of its states. This is in contrast to the light quark sector where states are broad and tend to mix. The states below the open charm threshold are well described by the quark model, but the spectrum above it is far for being understood. The are many states predicted by the quark model that have not been discovered yet and, in particular, there are plenty of unexpected states, the so called, XYZ states [4]. The XY states are candidates for exotics, such as hybrid states, *i.e.* a bound $c\bar{c}$ state with a gluonic component, molecules or tetraquarks but could also, in principle, be ordinary $\bar{c}c$ sates. All of them can, however, not be ordinary quark model states. The Z states are manifestly of exotic nature and antiproton annihilations are gluon rich processes which provides an excellent hunting ground for hybrids and glueballs. Many of these states are in the vicinity of open charm meson thresholds. This raises the question whether those states are of a $D^{(*)}\bar{D}^{(*)}$ molecular origin. Present experiments can not distinguish between different interpretations of the nature of these states. $\bar{\text{P}}$ANDA has the unique opportunity to make a difference here. The excellent momentum resolution of the $\bar{p}$ beam allows for a precise energy scan over states to determine their line shapes. One example is the $X(3872)$, also denoted as $\chi_{c1}(3872)$, whose mass lies at the $D\bar{D}^*$ threshold. A molecular state would make the line-shape asymmetric of the Flatté type due the coupling between the neutral and charged $D\bar{D}^*$ states whereas an ordinary $c\bar{c}$ state would yield a symmetric Breit-Wigner shape [5] as depicted in Figure 3.

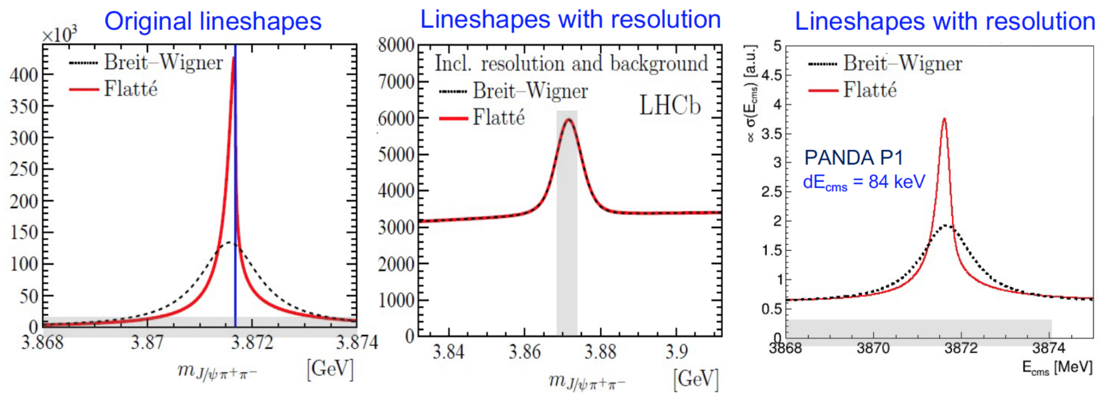

Figure 3. Comparison between the Breit-Wigner and Flatté-like lineshapes without (left), with the LHCb experiment [6] (middle) and $\bar{\text{P}}$ANDA resolutions convolved [7] (right).

3.2. Nucleon structure

Most information on the hadron internal structure has been obtained with the help of electromagnetic probes for which the structure is expressed in terms of form factors and structure functions. For spin $= 1/2$ particles is the form factor expressed in terms of an electric $G_E(q^2)$ and a magnetic $G_M(q^2)$ form factor as a function of the four-momentum squared, q^2. They are Fourier transforms of the charge and magnetisation densities, respectively, in the Breit frame for scattering processes (space-like region) where $q^2 < 0$. With $\bar{\text{P}}$ANDA one can study the $\bar{p}p \to e^+e^-, \mu^+\mu^-$ processes, *i.e.*, the proton form factor in the time-like where $q^2 > 0$. This will improve the world data [8] and the muon channel is unique for $\bar{\text{P}}$ANDA, for which lepton universality can be checked [9]. This provides additional information on the proton electric and magnetic current distributions since the space- and time-like regions are connected *via* dispersion relations. Furthermore, perturbative QCD (pQCD) predicts that G_E and G_M should become equal for the space- and time-like regions as $| q^2 | \to \infty$. This allow to check if the onset of pQCD happens within the energy range of HESR.

For Day 2 are several structure functions accessible, such as transition distribution amplitudes

(TDAs) via $\bar{p}p \rightarrow \gamma^{*}\pi^{0} \rightarrow e^{+}e^{-}\pi^{0}$, generalised distribution amplitudes (GDAs) via $\bar{p}p \rightarrow \gamma\gamma$, and parton distribution functions (PDAs) *via* $\bar{p}p \rightarrow (e^{+}e^{-}, \mu^{+}\mu-)X$ [2].

3.3. Strangeness physics

3.3.1. Hyperon production in $\bar{p}p \rightarrow \bar{Y}Y$ reactions

Exclusive production of strange antihyperon-hyperon pairs offers unique opportunities to study the strong interaction in the strange quark sector. The weak and parity violating decay of most hyperons gives access to polarisation and spin correlations in strangeness production. So far, high-quality data only exist for single-strange hyperons in the threshold region from the PS185 experiment [10, 11]. Only a handful of events exist for the doubly strange $\overline{\Xi^{-}}\Xi^{-}$ and $\overline{\Xi}^{0}\Xi^{0}$ channels [12] and nothing is known about the triple strange $\overline{\Omega^{-}}\Omega^{-}$ channel. One observation from PS185 was that the $\bar{\Lambda}\Lambda$-pair is produced in a triplet state [10], indicating that the $\bar{s}s$-pair is produced in triplet state. Are the Ξ:s also produced in a singlet state? $\bar{\text{P}}$ANDA will tell.
The large cross section for the $\bar{p}p \rightarrow \bar{\Lambda}\Lambda$ reaction as shown in Figure 4 allows for world leading statistics to be collected already at Day 1 after one day of data taking. This allows for a test of CP-violation in the $\bar{\Lambda}/\Lambda$ decay since the polarisation for the $\bar{\Lambda}$ should be equal but with opposite sign to the Λ if CP is conserved. This reflects the decay asymmetry parameter, α. From this, one defines $A_{CP} = (\alpha + \bar{\alpha})/(\alpha - \bar{\alpha})$ for which a non-zero value would indicate CP-violation. The doubly-strange Ξ^{-} is another interesting hyperon in the search for CP-violation. Here, its sequential decay $\Xi^{-} \rightarrow \Lambda\pi^{-} \rightarrow (p\pi^{-})\pi^{-}$ with its two parity violating weak decays give access to the additional decay asymmetry parameters β and ϕ. From these one can obtain similar asymmetries B_{CP}, B'_{CP} from β $\bar{\beta}$ as well as $\triangle\phi$. These quantities are more sensitive to CP violation by a factor of 100 and 10, respectively [13]

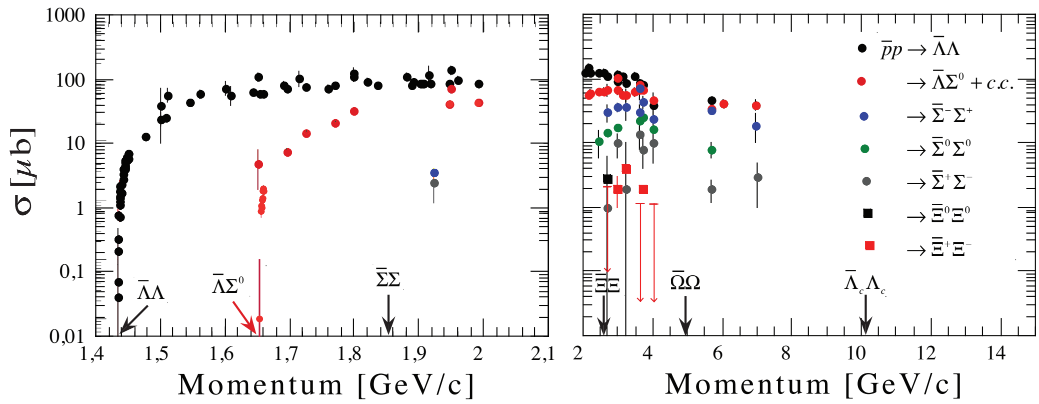

Figure 4. The world data of total cross sections for the $\bar{p}p \Rightarrow \overline{Y}Y$ reaction [10]. The different thresholds are indicated by arrows.

3.3.2. Hyperon spectroscopy Baryon spectroscopy was decisive for the for the formulation of the quark model. It is successful in describing the baryon ground state properties but fails to explain many features of their excitation spectra. To shed more light on the properties of excited baryons more data are needed. This is particularly true for multiple strange hyperons. Very few excited states of Ξ's have been observed and nothing is known about excited Ω's [14]. The high production rate of strangeness in $\bar{p}p$ collisions makes the $\bar{\text{P}}$ANDA experiment an excellent tool to search for excited double- and triple-strange hyperons and pin down their quantum numbers.

3.3.3. Hyperatoms and hypernuclei For Day 2 $\bar{\text{P}}$ANDA will have the possibility to replace the tracking part of the TS with a detector set-up designed to measure hyperatoms and hypernuclei. Here, Ξ^-'s will be produced in a C target and subsequently decelerated and stopped in a secondary target. The X-rays from the atomic cascade of captured Ξ^-'s in a Pb target will be measured in a Ge-detector array. Double Λ-hypernuclei will be produced in a Be target via the $\Xi^- p \to \Lambda\Lambda$ capture process. The strong interaction shift and width in the Ξ^--Pb data will probe the Ξ^- with the neutron skin. γ-rays from excited $Be_{\Lambda\Lambda}$ nuclei will give important information on the Λ nuclear potential as well as the Λ-Λ interaction in the nuclear medium [15]. This will provide important input for the modelling of the interior of neutron stars and its hyperon puzzle.

3.4. Hadrons in nuclei

The study of antihyperon production on nuclei offers a unique way to reveal strong in-medium effects generated by the attractive antihyperon-nucleus potential, but no data exist today. $\bar{\text{P}}$ANDA can provide such information from exclusive $\overline{Y}Y$ production in $\bar{p}A$ reactions close to threshold since the transverse momentum asymmetry between the $\overline{Y}$ and Y is sensitive to the $\overline{Y}A$ potential [16].

The production rate of J/ψ as a function of the mass number in $\overline{p}+A \to J/\psi+(A-1)^*$ will give important information on the J/ψ interaction with in nuclear matter and the quest of nuclear transparency in relativistic heavy-ion collisions [2].

4. Conclusions

$\bar{\text{P}}$ANDA is a unique facility that uses modern detector technologies to carry out a broad physics program employing antiprotons. The program covers important and timely aspects of nuclear, hadron and particle physics across the transition from nucleons to elementary quarks with a large discovery potential.

5. References

[1] The PANDA Collaboration 2005 PANDA Technical Progress Report *FAIR-ESAC*
[2] Erni W *et al.* (PANDA Collaboration) 2009 arXiv:0903.3905
[3] Lutz M F M *et al.* 2016 *Nucl. Phys.* A **948** 93
Barucca G *et al.* 2021 (PANDA Collaboration) Eur. Phys. J. A **57** 184
[4] Olsen *et al.* 2018 *Rev. Mod. Phys.* **90** 015003
Brambilla S *et al.* 2020 *Rhys. Rep.* **873** 1
Mezzadri G and Spataro S 2022 *Rev. in Phys* **8** 100070
[5] Haidenbauer C *et al.* 2007 *Phys. Rev.* D **76** 034007
[6] Aaij R *et al.* (LHCb Collaboration) 2020 *Phys. Rev.* D **102** 092005
[7] Nerling F 2021 *PoS CHARM2020* 004
[8] Singh B *et al.* (PANDA Collaboration) 2016 *Eur. Phys. J.* A **52** 325
[9] Barucca G *et al.* (PANDA Collaboration) 2021 *Eur. Phys. J.* A **57** 30
[10] Johansson T 2005 *Proc. Eight Int. Conf. on Low Energy Antiproton Physics (LEAP'05) AIP Conf. Proc.* **796** 96
[11] Barnes P D 1991 *et al. Nucl. Phys* A **526** 575
Barnes P D 2000 *et al. Phys. Rev.* C **62** 055203
Paschke K 2006 *et al. Phys Rev.* C **74** 015206
[12] Musgrave B and Petmezas S 1965 *Nuovo Cim.* **35** 735
Baltay C 1965 *et al. Phys Rev.* B **140** 1027
[13] Donogue J F 1995 *et al. Phys Rev.* D **74** 3927
[14] Workman R L *et at.* 2022 *Prog. Theor. Exp. Phys.* 083C01
[15] Singh B *et al.* (PANDA Collaboration) 2016 Nucl. Phys. A **954** 323
[16] Pochodzalla J 2008 *Phys. Lett.* B **669** 306